Eur. Phys. J. A **4**, 335–341 (1999)

THE EUROPEAN PHYSICAL JOURNAL A
© Springer-Verlag 1999

Fine structure in ^{14}C cluster emission from ^{225}Ac

M. Mirea

Institute of Physics and Nuclear Engineering, Tandem Lab., P.O.Box MG–6, Bucarest, Romania

Received: 31 July 1998 / Revised version: 27 November 1998
Communicated by D. Guerreau

Abstract. A fine structure in the ^{14}C decay of ^{225}Ac is predicted quantitatively by accounting dynamical aspects during the disintegration process. Transitions to the excited states of the daughter nucleus are considered to be mainly directed by the Landau–Zener promotion mechanism in the region of avoided crossing levels. The level scheme is evaluated with the superasymmetric two–center shell model. The half–lives are computed considering the cluster decay as a superasymmetric fission process.

PACS. 23.70.+j Heavy-particle decay – 21.60.Cs Shell model – 21.60.Gx Cluster models – 24.75.+i General properties of fission

1 Introduction

The cluster decay was predicted in 1980 [1] within a quantum mechanical fragmentation theory and experimentally evidenced in 1984 [2,3]. Few time later, a fine structure in cluster emission was also anticipated [4–6]. Exploiting the unique qualities of the SOLENO spectrometer, the Orsay group discovered a fine structure in the energy spectrum concerning the ^{14}C decay from ^{223}Ra [7,8], characterized by a more intense branch to the first single–particle excited state of the daughter ^{209}Pb. Theoretical investigations were effected emphasizing the similarity with the same phenomenon observed in the alpha decay [9] of odd–A reflection–asymmetric deformed nuclei [10–12]. By calculating the overlaps between the $\frac{3}{2}^+$ orbital of the unpaired neutron in the ground state of the ^{223}Ra and the orbitals for a spherical shape (assumed to characterize the daughter ^{209}Pb), it was pointed out that the main component is $i_{11/2}$ with small admixtures from $g_{9/2}$ and $j_{15/2}$. This result is quantitatively consistent with the favored decay to the $\frac{11}{2}^+$ state in ^{209}Pb if the variations of the Gamow factor between different channels are neglected. In a more realistic way, calculations of hindrance factors were performed within the one level R–matrix approximation [13,14]. The fine structure phenomenon was also analyzed through models inspired from alpha decay theories [15–17] or fission–like ones [18,19]. An extended overview of these microscopic theories can be found in [20].

In a competitive way, the experimental result was also explained appealing to the Landau–Zener promotion mechanism, i.e., considering an enhancement of transition probabilities of the unpaired nucleon during the disintegration process in the avoided level crossing regions. The role played by the Landau–Zener effect in cluster decays was evidencied in [21,22] and, quantitatively, the theoretical results display an excellent agreement with the experimental values. In this context, the same formalism is exploited for the study of the ^{225}Ac$\rightarrow^{14}$C+^{211}Bi decay in oder to predict quantitatively the fine structure characteristics.

This system was chose because an experimental value of the hindrance factor will provide spectroscopic information about the controversial ^{225}Ac nucleus [23]. Moreover, with magnetic spectroscopy, Hussonnois hopes to be able to measure the kinetic energy of the ^{14}C accurately enough to infer the levels of the ^{211}Bi [24,25] in the near future.

2 Formalism

As in the previous work [21,22] the deformations of the nuclei are neglected. To avoid the use of different least action trajectories in the configuration space required by each reaction channel, a simple nuclear shape parametrization, given only by the intersection of two spheres with different radii, is used. So, the single degree of freedom becomes the elongation R, denoting the distance between the two centers of the fragments. The mass–asymmetry is determined during the decay by using a constant value of the emitted fragment radius. A normalized coordinate of elongation $R_{\rm n} = (R - R_{\rm i})/(R_{\rm f} - R_{\rm i})$ is also used, where $R_{\rm i} = R_{0\rm s} - R_{2\rm s}$ characterizes the geometry at the initial moment of the decay, given by two overlapping tangent spheres, $R_f = R_{1\rm s} + R_{2\rm s}$ denotes the elongation for the configuration of two external tangent spheres, $R_{i\rm s} = 1.16\ A_i^{\frac{1}{3}}$ with $i = 0, 1, 2$, being the radii of the parent, the daughter and the emitted nuclei considered spherical, respectively.

The adiabatic levels are obtained with an improved version of the superasymmetric two–center shell model

(STCSM) [26], inspired from [27]. The Hamiltonian (in cylindrical coordinates) is split into several parts which are treated separately:

$$V(\rho,z,\varphi) = V_0(\rho,z) + V_{as}(\rho,z) + V_n(\rho,z) + V_{Ls}(\rho,z,\varphi) + V_{L^2}(\rho,z,\varphi) - V_c \quad (1)$$

where $V_0(\rho,z)$ is the two–center potential which eigenvectors can be solved analytically, $V_{as}(\rho,z)$ is the mass–asymmetry term having the improved form described in details in [22] and $V_n(\rho,z)$, $V_{Ls}(\rho,z,\varphi)$, $V_{L^2}(\rho,z,\varphi)$, V_c are correction terms related to the necking, to the spin-orbit and $\mathbf{L}^2$ couplings and to the depth of the potential, respectively. The description of these correction terms can be found in [26]. The used values of the coupling constants are determined in order to reproduce the real level scheme and are κ=0.051851, κ_1 =0.0547581, κ_2=0.1345, μ =0.6445597, μ_1=0.5686 and μ_2=1.16365. The depths of the potentials are V_c=48.925, V_{c1}=49.0804 and V_{c2}=53.99. The values of the coefficients κ, μ and V_c, entering in the Hamiltonian are deduced for a spherical ^{225}Ac by χ^2–fitting the single particle levels obtained with a realistic Wood–Saxon potential [28] found in the neighboring of the Fermi energy. The values which characterize the ^{211}Bi–coefficients are determined using the same fit procedure applied to available experimental data [29]. Finally, the values assigned to ^{14}C are computed by meaning the coupling constants determined for light nuclei as ^{15}N, ^{13}N and ^{13}B using level schemes found in [30]. In general, three or four spherical levels above and under the Fermi energy were accounted and some inevitable minor differences between the energetic values of the levels obtained with our modified oscillator model and the experimental reference values arise. For example, the experimental value of the first excited state of ^{211}Bi is 0.404 MeV while from our microscopic level scheme, the theoretical value becomes 0.46 MeV. However, all the theoretical calculations are made using as reference the theoretical level scheme, that means, even the penetrabilities relative to the excited state are calculated according with the single–particle differences in energies deduced from the theoretical level scheme. Here, the cutoff value of the major quantum number is chose $N_{\max}$=10. In principle, the resulting level scheme keeps the principal trends (number of avoided level crossings) unchanged as long as the modifications of the two–centre shell model parameters do not transform the succession of the order of the levels. In Fig. 1, the energetic proton level scheme is displayed as function of the elongation R_n. The the single particle levels are labeled by their spectroscopic notations, on the left side, for the parent, and, on the right side, for the daughter and the emitted nucleus, in the first and second column, respectively. In the following text, the superscript H is added for the heavy fragment.

As evidenced in [23], to treat the reaction ^{225}Ac$\rightarrow^{14}$C+^{211}Bi, two assignments can be taken into consideration concerning the unpaired proton with spin Ω =3/2 [31] if the parent ^{225}Ac is in ground state. The first one [29] considers that the proton is located in the orbit which emerges from the spherical subshell $1h_{9/2}$ while the second assent claims that the last unpaired nucleon originates [32] from the $2f_{7/2}$ spherical orbital. Let consider that in the Ac ground state, the unpaired proton is located somewhere on the level emerging from $1h_{9/2}$, the system being characterized by a R_n included in an interval large enough around zero to include the possible deformations of the parent. An overview on the level scheme presented in Fig. 1 reveals that this first hypothesis leads to a very unfavorable energetic configuration of the daughter after the disintegration, the unpaired proton reaching adiabatically the state $1h^H_{11/2}$, resulting a hole configuration. So, this proposed assignment for the unpaired proton in the ground state of the parent leads to a hindered process from energetic conditions. Moreover, an excitation to the superior level with same spin Ω =3/2, i.e., the level emerging from $2f_{7/2}$ is not allowed because of the non-existence of pronounced avoided crossings between these levels during the decay. The second hypothesis seems to be more realistic, leading adiabatically to a final ground state configuration of the unpaired nucleon in the $1h^H_{9/2}$ spherical orbital. This discussion persuades us to consider that ^{225}Ac has the spin $\frac{3}{2}$ emerging from $2f_{7/2}$ as considered in [32]. In the following, the fine structure of the ^{14}C radioactivity can be understood by an enhanced transition probability of the unpaired neutron from the adiabatic level with $\Omega = \frac{3}{2}$ emerging from $2f_{7/2}$, to the superior adiabatic levels with the same spin projection emerging from $1i_{13/2}$ and $2f_{5/2}$, according with the Landau–Zener effect.

The realistic two–center level diagram presented before provides an instrument to study the role of individual orbitals during the disintegration process in a similar way as the study of nucleus–nucleus collision [33]. The molecular levels are functions of the internuclear distance. Levels with the same symmetry cannot cross during an adiabatic process and exhibit avoided level crossings. The point of nearest approach between two such levels is known as avoided level crossing. If the internuclear distance varies, the transition probability of a nucleon between two adiabatic levels is strongly enhanced in the region of avoided crossings. This promotion mechanism is generically entitled the Landau–Zener effect. This effect was used since 1980 [34] in light heavy ion reactions to predict single–particle excited states after collisions.

Adiabatically, for Ω=3/2, the level scheme presented in Fig. 1 shows that the $1h_{9/2}$ level reaches the $1h^H_{11/2}$ state, the $2f_{7/2}$ level reaches the $1h^H_{9/2}$ state, the $1i_{13/2}$ level reaches the $2f^H_{7/2}$ state and the $2f_{5/2}$ level reaches the $1i^H_{13/2}$ state of the ^{211}Bi daughter considered spherical. Our goal is to compute the occupation probabilities of the unpaired proton in the three levels corresponding to the ground state and the first two single–particle excited state ($2h^H_{9/2}$, $2f^H_{7/2}$ and $1i^H_{13/2}$) in the final stage of the disintegration process using the Landau–Zener promotion mechanism. Two avoided crossings can participate to the one–body excitations. To show that, the diabatic levels emerging from $2f_{7/2}$, $1i_{13/2}$ and $2f_{5/2}$ are denoted with ϵ_1, ϵ_2 and ϵ_3, respectively. At the beginning the $2f_{7/2}$ is

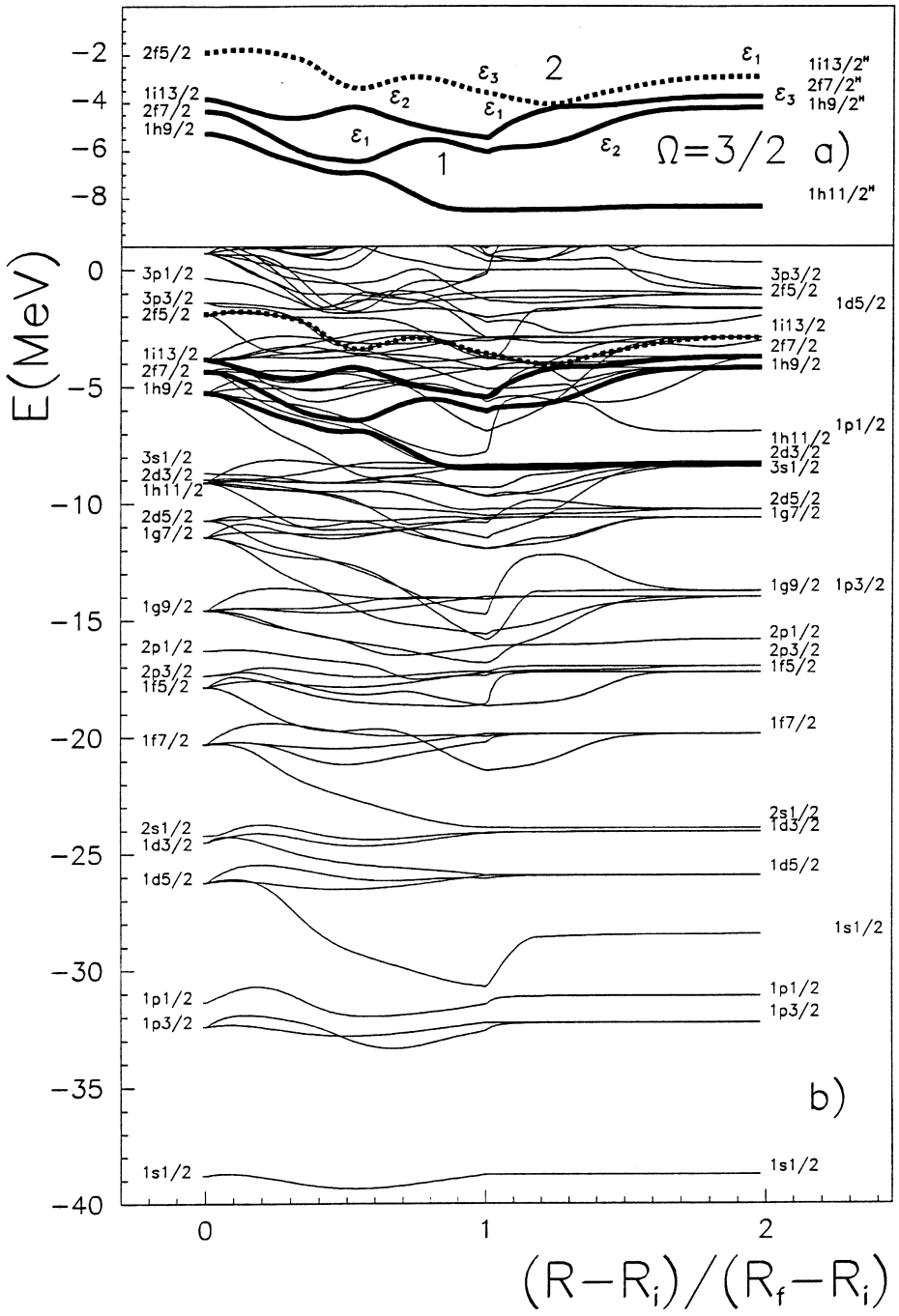

Fig. 1. Protonic level scheme for the ^{14}C spontaneous emission from ^{225}Ac with respect to the normalized elongation. The levels emerging from $1h_{\frac{9}{2}}$, $2f_{\frac{7}{2}}$ and $1i_{\frac{13}{2}}$ are plotted with thick lines and that from $2f_{\frac{5}{2}}$ with a dotted line. a) Detailed part of the level scheme where only the levels with Ω=3/2 are plotted and the avoided level crossings are numbered. b) Total level scheme. At the beginning, the behavior is similar to a Nilsson diagram for prolate deformations

filled with a proton. During the decay, a first avoided crossing which can excite the proton is localized at $R_n \approx 0.9$ between the diabatic states ϵ_1 and ϵ_2. After the passage through this region ϵ_1 is assimilated to the adiabatic level emerging from $1i_{13/2}$ and ϵ_2 is assimilated to that emerging from $2f_{7/2}$. The second avoided crossing can be remarked at $R_n \approx 1.2$ between the diabatic levels ϵ_1 and ϵ_3. After the passage through this second crossing region, ϵ_1 is assimilated to the adiabatic level emerging from $2f_{5/2}$ and ϵ_3 is assimilated to the adiabatic level emerging from $1i_{13/2}$. Finally, ϵ_1, ϵ_2 and ϵ_3 reach the final daughter orbitals $1i^H_{13/2}$, $1h^H_{9/2}$ and $2f^H_{7/2}$, respectively.

From now on, the same treatment as in [21,22] is performed. Assuming a three-state approximation by taking into account the three levels emerging from $2f_{7/2}$, $1i_{13/2}$, $2f_{5/2}$, the wave function of the unpaired neutron can be expanded [35,36] in a basis of three diabatic wave functions $\phi_i(\mathbf{r}, R)$ as

$$\psi(\mathbf{r}, R) = \sum_{i=1}^{3} c_i(t)\phi_i(\mathbf{r}, R) \exp\left[-\frac{i}{\hbar}\int_0^t \epsilon_{ii} \mathrm{d}t\right], \qquad (2)$$

where the matrix elements between the diabatic states ϕ are abbreviated by

$$\epsilon_{ij} = \langle \phi_i \mid H \mid \phi_j \rangle, \tag{3}$$

H being the Hamiltonian of STCSM. Inserting ψ into the time-dependent Schrödinger equation, the following coupled equations are obtained [21]:

$$\dot{c}_i = \frac{1}{i\hbar}\epsilon_{ij}\exp(i\alpha_{ij})c_j + \frac{1}{i\hbar}\epsilon_{ik}\exp(i\alpha_{ik})c_k, \quad i,j,k = 1,2,3, \tag{4}$$

with

$$\alpha_{ij} = \int_0^t (\epsilon_{ii} - \epsilon_{jj})\mathrm{d}t/\hbar. \tag{5}$$

The initial conditions are $c_1(t=0) = 1$, $c_2(t=0) = 0$, $c_3(t=0) = 0$. We need to know the values of $\epsilon_{ii} = \epsilon_i$, $\epsilon_{ij} = \epsilon_{ji}$, and the relative velocity $\dot{R}$. The kinetic energy available during the disintegration process is preserved and variations of the relative velocity $\dot{R}$ are due essentially to the modifications of the effective mass B_R. The inertia B_R with respect to the elongation is computed [37, 38] in the Werner–Wheeler approximation. In general, the so–called tensor of inertial coefficients B_{ij} (inertial parameters) contains information about the mode in which the nucleus reacts to the generalized forces acting on the nuclear shape. These generalized forces are depending on the deformation energy [39]. If the variables which define the shape of the effective nuclear surface are used also as collective variables (shape parameters of the potential) this tensor is also known as the tensor of effective mass parameters. The quantity B_R being calculated in the frame of the Werner–Wheeler method, its sense can be extended as effective mass parameters. The consistency condition is realised: the same shape for the macroscopic potential, for the microscopic one and for the tensor of inertial coefficients.

The system (4) is evaluated numerically using the Runge–Kutta formula. The three diabatic states are computed using spline interpolations around the level crossings and are denoted by ϵ_1, ϵ_2 and ϵ_3. The interaction matrix elements ϵ_{ij} between these diabatic states are a measure of differences between adiabatic and diabatic energies. A kinetic energy $E_k = 70$ keV is used because it was determined previously [21,22] that it provides a good fit for the ratio between experimental half-lives of the two ^{223}Ra parent nucleus decay modes experimentally confirmed in the fine structure phenomenon of ^{14}C emission. Asymptotically, the occupation probabilities values $p_{\epsilon_i} = \mid c_i \mid^2$, $i = 1,2,3$, of the diabatic levels are $p_{\epsilon_1} = 0.958$, $p_{\epsilon_2} = 4.1 \times 10^{-2}$ and $p_{\epsilon_3} = 1.1 \times 10^{-4}$. Consequently, at the exit point from the potential barrier, the unpaired neutron of the daughter has the probability p_{ϵ_1} to be in the second excited state $1i^H_{13/2}$, p_{ϵ_2} to be in the ground state $1h^H_{9/2}$ and the probability p_{ϵ_3} to be in the first excited state state $2f^H_{7/2}$.

The second single particle excited state given theoretically by the single particle scheme is not found experimentally in ^{211}Bi. Nevertheless, it can be interpreted that this formalism indicates that reaching the $1i^H_{13/2}$ orbital, the unpaired proton carries during the scission process enough energy (of the order of 1.3 MeV) to excite the daughter in higher energetic states (other experimental levels are found for 0.7663 MeV, 0.832 MeV and 6 values between 0.951 and 1.27 MeV) or even to emit the unpaired proton. In this last case, a simultaneous emission of the unpaired proton with the cluster decay is predicted. This is the way in that the second excited state must be understand.

The partial half–life of the channel i, is obtained with the equation

$$T^i_{1/2} = \frac{h\ln 2}{2E_{\mathrm{v}}S_i}\exp(K_i), \tag{6}$$

where E_{v} is the zero-point vibration energy (ZPE), S_i is the spectroscopic amplitude which has the same interpretation as p_{ϵ_i} and K_i is the action integral determined for the channel i. As explained in [20], the spectroscopic amplitude is the probability for the mother nucleus to be found in a state of the type of cluster and daughter nucleus. Considering that the resonance or decaying state are formally similar to a bound state, the spectroscopic amplitude can be calculated classically as the projection of the mother state onto the product of states of the two fragments. A quantity which has the same interpretation as the spectroscopic amplitude is obtained using the Landau–Zener effect, but its calculation is effected by taking into account dynamical effects during the disintegration process. In the case of even-even nuclei, S=1. The action integral is calculated by using the semi-classical Wentzel-Kramers-Brillouin (WKB) approximation being computed for a given energy which connects one point in the ground state and the exit point of the barrier [39]. This energy is determined in our case by the value $Q + E'_{\mathrm{v}}$, where E'_{v} is a fraction of the ZPE lost to surpass the barrier. The excitations of the system in the avoided crossing regions are translated in an increase of the potential barrier, E'_{v} being unmodified. The phenomenologic deformation energy E^0_{d} is computed in the framework of the Yukawa-plus-exponential model [40] extended for binary systems with different charge densities including phenomenological shell corrections [41] and diffuseness correction to Coulomb potential [38] as in the numerical superasymmetric fission model. $E'_{\mathrm{v}} + E_{\mathrm{k}} = E_{\mathrm{v}} = 0.44$ MeV according with [41]. It is assumed that the deformation energy E^0_{d} is a good approximation to the adiabatic potential energy surface of even–even nuclei. So, it can be considered that $E_{\mathrm{d}} = E^0_{\mathrm{d}}$ for ground state. The Q–values are obtained from [42]. The specialization energy for ^{225}Ac is added to the potential barrier in the same manner as in Refs [21,22]. For an even-odd nucleus, if the system is not excited, the specialization energy [43] explains the energy excess of the nucleus during the decay with respect to a given spin of the unpaired nucleon. The specialization energy is defined as the excess of the energy of a nucleus having an unpaired nucleon characterized by a given spin–parity versus the energy of the same nucleus, at the same deformation, with the nucleon in a same spin–parity state of lowest energy. It is precised in [43] that this difference in energies may be considered to measure the amount by which the fission barrier for an odd nucleus exceeds that for a neighboring even–even nucleus. In our calculations,

the parity content of given single–particle state change along the deformation path due to the mass–asymmetry. Therefore, the energy excess is related only to nucleons with same spin Ω and this specialization energy is translated in an increase of the potential barrier during the disintegration process in the avoided crossing regions. The action integral is approximated by the formula:

$$K_i = \frac{2}{\hbar}\int_{R_i^{\text{g.s.}}}^{R_e^i} [2B_R(R)(E_d^i(R) - Q_{\text{g.s.}} - E_v')]^{1/2} dR \quad (7)$$

where $R_i^{\text{g.s.}}$ is the first turning point, R_e^i is the second turning point (depending on the specialization energy), E_d^i is the deformation energy obtained by adding to E_d^0 the specialization energy.

Only a three level approximation is sufficient to treat this decay mode if the unpaired proton is initially considered to lie in the level with spin Ω=3/2 emerging from $2f_{7/2}$ at a non-zero deformation of the ^{225}Ac parent. In this case, the level emerging from $1i_{7/2}$ is empty and the avoided crossing with the level emerging from $2f_{5/2}$ produced at $R_n \approx 0.5$ can not produce single–particle transitions. The involved level with greatest energy emerging from $2f_{5/2}$ can be filled only at the second avoided crossing located at $R_n \approx 1.2$, afterwards, this level reaches smoothly its final state $1i_{13/2}^H$ without existence of conditions for another single–particle transition.

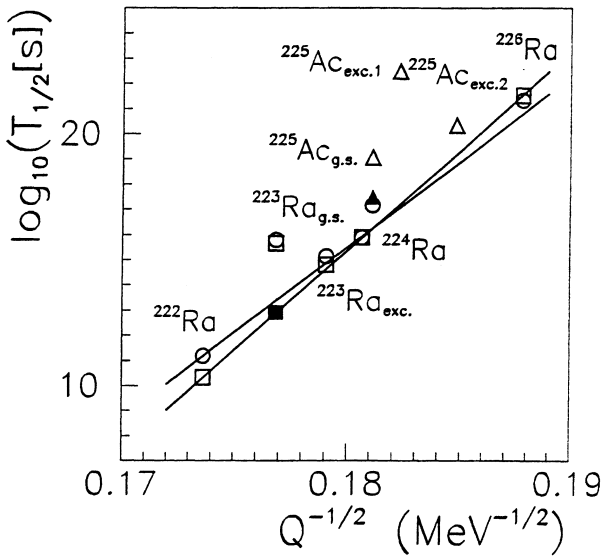

Fig. 2. Theoretical and experimental values of the total and partial half–lives relative to cluster decay in a Geiger–Nutall plot. The experimental values of the total half–lives for the ^{14}C emission from ^{222}Ra,^{224}Ra,^{226}Ra [22], ^{225}Ac [21] and the partial values of the half–lives from ^{223}Ra [8] are displayed with empty circles. The theoretical values for the ^{14}C emission from Ra [19] are plotted with empty squares while the theoretical values concerning the ^{225}Ac parent are represented with empty triangles. A filled square and a filled triangle refer to the theoretical values obtained without taking into consideration the Landau–Zener effect. The Q–values are obtained from [39]

3 Results and discussion

With the assumption that the ZPE is the energy available during the disintegration, its value can be divided in two parts, one part (E_{v}') is lost as a potential energy in the attempt to surpass the potential barrier and the rest (E_{k}) participates as a kinetic energy of the whole system. The two turning points of the potential barrier exhibit the same energy, so, the fraction of the ZPE given by the kinetic energy keeps a constant value and intrinsic excitations are translated in the increase of the potential barrier. Two opposite effects are competitive when the kinetic energy is increased: the asymptotic occupation probability of the excited states is enhanced but, in the same time, the penetrability is diminished because the fraction of the ZPE used to surpass the barrier is decreased. This diminution of the penetrability is more marked for the excited channel since the potential barrier is larger than that of the ground state.

Finaly, the calculation show that the probability to have the unpaired proton in the first excited state of the daughter ^{211}Bi is hindered. The ratio between the half-lives of the channel with the daughter in the ground state to that in the first excited state being almost 4. $\times 10^{-4}$. It is possible to have a second excited state or proton emission during the decay with a branching ratio of 0.042 relative to the ground state. The second single particle excited state must be understood in the sense that the proton carries enough energy to excite superior levels of the nucleus or for proton emission. These results are almost independent of the model used to compute the partial half–lives and are essentially determined by mean of the Landau–Zener promotion mechanism.

Both theoretical and experimental Geiger–Nuttal plots for both reactions ^{223}Ra $\rightarrow ^{14}$C + ^{209}Pb and ^{225}Ac $\rightarrow ^{14}$C + ^{211}Bi are represented in Fig. 2. The preexponential factor $h\ln(2)/2E_{\text{v}}$ in the Rel. (6) used to compute the half–lives presented in this figure is obtained for all the theoretical results to be given by the ratio between the experimental half–life for the ^{14}C decay of ^{224}Ra and the Gamow factor of the same reaction.

All theoretical values of the Gamow factors are determined in the frame of the numerical superasymmetric fission model, accounting phenomenological shell effects by adjusting the theoretical Q–value of the decay by a fitting procedure as in [41] in order to reproduce the experimental one. Therefore, the total half–life of the ^{225}Ac is well reproduced when the Landau–Zener effect is not accounted and the transitions are considered to be produced only from the ground state of the parent to the ground state of the daughter (the filled triangle in Fig. 2). If the Landau–Zener is introduced, the different channels (referred as transitions on different excited states of the daughter) are characterized by different probabilities (already denoted with p_{ϵ_i}) and greater values of the Gamow factor than that of the ground state. The simultaneous variations of these two ingredients are translated

in a higher theoretical total half–life

$$T_{1/2}^{\rm total} = \frac{1}{\sum_i \frac{1}{T_{1/2}^i}} \quad (8)$$

than that given by the filled triangle in Fig. 2. Therefore, to estimate realistic values of the hindrance factors and of the partial half–lifes we use the Rel. (8) where $T_{1/2}^{\rm total}$ is replaced with the experimental value, having in mind that the ratios between the different partial half–lives are obtained from the spectroscopic factors determined before and their respective penetrabilities. This renormalization was not used in the calculations effected for ^{14}C decay of ^{223}Ra because the theoretical value of the total half–life without Landau–Zener effect (filled square in Fig. 2) was much smaller than the experimental one. The hypothetical half–lives deduced from the Geiger–Nuttal plot are obtained from the straight line between the experimental half–lives of ^{224}Ra and ^{226}Ra and have the following values in seconds: 1.88 $\times 10^{16}$, 1.50 $\times 10^{17}$ and 1.12 $\times 10^{19}$, for the ground state and the first two successive excited states, respectively. For the same sequence, the theoretical deduced half–lives in seconds are: 1.38 $\times 10^{17}$, 3.45 $\times 10^{20}$ and 3.29 $\times 10^{18}$. So, the hindrance factor for the ground state is 7.34, for the first excited state is 2306 and for the second excited state (in the sense that this second single particle excited state contains enough energy to excite the superior levels or to emit a proton as remarked in Sect. 2) is 0.3.

This process was also analyzed quantitatively in [44] where the half–life is determined with a preformation probability deduced from a straight line approximation. Comparison with the experimental total half–life for this decay leads to consider that the ground state to ground state transitions are favored. Also, with the analytical superasymmetric fission model it was deduced that the transitions to the ground state of the daughter are not hindered [18]. These predictions are in qualitative agreement with the calculations presented in this paper. Quantitatively, for example, the calculations presented in [16] show that the intensity to the ground state is only 5 times greater than that to the first excited state of the daughter. Here, structure ingredients are not included, the half–lives of different channels being mainly obtained by adjusting the Q–value. None of these predictions expect a low hindrance factor for higher excited states.

This formalism can be considered as a fine structure in the rate of cluster decay. Some simple arguments in analogy with the results obtained in [45,46] can be given in favor of the semi–classical approximation presented in this paper. In these references, at the initial moment a metastable state of the parent is generated and a wave function "begins" to advance through the potential barrier. The probability ρ to find the system beyond a configuration defined by a elongation r of the system and the alpha decay rate λ are time–dependent parameters. Their calculations show that after a short period of time (the transient time) the alpha decay rate reaches a mean value characterized, however, by small oscillations around this mean value, the quasi–stationary regime being obtained. The period of these small oscillations is almost constant in this quasi–stationary regime. Important is that this mean quasi–stationary value of the decay rate is almost equal to the decay rate obtained from the classical penetrability theorem, that means the value used in the present work to define the half–lives. The small oscillations around the mean value determine the tunneling time, that means, the time lost by the maximum of these oscillations to arrive from the first turning point to the second one. This value is fitted reasonably in the calculations presented in this paper: for alpha decay, the time of tunneling given in the above references is of the order of (10^{-21}–10^{-22}) s while in this work a tunneling time of the order of 10^{-20} s can be deduced for cluster decay. Further, the quasi–stationary regime can be approximated by the classical Gamow picture. So, if the Gamow description is a good approximation of the time dependent behavior, there are no reasons to not introduce the tunneling time in the semi–classical formalism.

Apart the work of Dumitrescu [13], the other models do no take into consideration the residuals effects. Even in the work of Dumitrescu some approximations were inevitables because it is not possible to handle accurately the very complicated formulae generated by accounting residual effects in the R–matrix formalism. Therefore, he used only a diagonal interaction and one dominant term in the spectroscopic amplitudes, the real effects being partially lost. All the other articles used very crude approximations, and apart the simple interpretations based on overlap calculations between orbitals, even the simple single–particle structure is neglected. The description presented in this work accounts for single–particle effects and the dynamic of the process.

The fine structure phenomenon is explained appealing essentially to two ingredients: the Landau–Zener effect and the specialization energy. Both of them producing opposite effects which weaker the ratio between the partial half–life of the cluster decay to the ground state and that of the first excited states. When the kinetic energy is increased, the excitations on superior levels due to Landau–Zener effect are enhanced while the penetrabilities are decreased accordingly, by increasing the barrier. This treatment also provides a different way to attack the fine structure phenomenon by accounting dynamically single–particle energetic trends during the process.

I thank Professor M. Hussonnois for illuminating discussions. This work was partially supported by a Romanian Academy Grant (75/98).

References

1. A. Săndulescu, D.N. Poenaru and W. Greiner, Sovt. J. Nucl. **11** (1980) 528
2. H.J. Rose and G.A. Jones, Nature **307** (1984) 245
3. D.V. Aleksandrov, A.F. Belyatskii, Yu.A. Glukhov, E.Yu. Nikol'skii, B.G. Novatskii, A.A. Oglobin and D.N. Stepanov, JETP Lett. **40** (1984) 909

4. M. Greiner and W. Scheid, J. Phys. G: Nucl. Part. Phys. **12** (1986) L229
5. W. Henning and W. Kutschera, in *Particle Emission from Nuclei*, edited by D.N. Poenaru and M.S. Ivaşcu (CRC Press, Boca Raton, 1989), vol. II, chap. 7, pp. 189
6. I. Silişteanu and M. Ivaşcu, J. Phys. G: Nucl. Part. Phys. **15** (1989) 1405
7. L. Brillard, A.G. Elayi, E. Hourani, M. Hussonnois, J.F. Le Du, L.H. Rosier and L. Stab, C. R. Acad. Sci. Paris **309** (1989) 1105
8. E. Hourany, G. Berrier-Ronsin, A. Elayi, P. Hoffmann-Rothe, A.C. Mueller, L. Rosier, G. Rotbard, G. Renou, A. Liebe, D.N. Poenaru and H.L. Ravn, Phys. Rev. C **52** (1995) 267
9. S. Rosenblum, C. R. Acad. Sci. Paris **188** (1929) 1401
10. M. Hussonnois, J.F. Le Du, L. Brillard and G. Ardisson, J. Phys. G: Nucl. Part. Phys. **16** (1990) L77; Phys. Rev. C **44** (1991) 2884
11. M. Hussonnois and G. Ardisson, Z. Phys. A **349** (1994) 311
12. R.K. Sheline and I. Ragnarsson, Phys. Rev. C **43**, 1476 (1991); **44** (1991) 2886; **55** (1997) 732
13. O. Dumitrescu, Phys. Rev. C **49** (1994) 1466; O. Dumitrescu and C. Cioaca, *ibid* **51** (1995) 3264
14. R. Bonetti, I. Bulboacă, F. Cârstoiu and O. Dumitrescu, Phys. Lett. B **396** (1997) 15
15. R. Blendowske, T. Fliessbach and H. Walliser, Z. Phys. A **339** (1991) 121
16. B. Buck, A.C. Merchand and S.M. Perez, Nucl. Phys. A **512** (1990) 483
17. Raj. K. Gupta, M. Horoi, A. Săndulescu, M. Greiner and W. Scheid, J. Phys. G: Nucl. Part. Phys. **19** (1993) 2063
18. D.N. Poenaru and W. Greiner, in *Nuclear Decay Modes* edited by D.N. Poenaru (Institute of Physics Publishing, Bristol and Philadelphia, 1996) pp. 317
19. D.N. Poenaru, E. Hourani and W. Greiner, Ann. Physik **3** (1994) 107
20. R.G. Lovas, R.J. Liotta, A. Insolia, K. Varga and D.S. Delion, Phys. Rep. **294** (1998) 265
21. M. Mirea and F. Clapier, Europhys. Lett. **40** (1997) 509
22. M. Mirea, Phys. Rev. C **57** (1998) 2484
23. R. Bonetti, C. Chiesa, A. Guglielmetti, R. Matheoud and C. Migliorino, Nucl. Phys. A **562** (1993) 32
24. G. Ardisson and M. Hussonnois, Radiochimica Acta **70/71** (1995) 123
25. P.B. Price, in *Frontier Topics in Nuclear Physics*, edited by W. Scheid, A. Sandulescu (Plenum Press, New York, 1994), p. 39
26. M. Mirea, Phys. Rev. C **54** (1996) 302
27. J.A. Maruhn and W. Greiner, Z. Phys. **251** (1972) 431
28. S. Cwiok, J. Dudek, W. Nazarewicz, J. Skalski and T. Werner, Comp. Phys. Comm. **46** (1987) 379
29. E. Browne, J.M. Dairiki, R.E. Doebles, A.A. Shibab–Eldin, L.J. Jardine, J.K. Thuli and A.B. Buyrni, in *Tables of isotopes*, edited by C. Michael Lederer and Virginia S. Shirley (John Wiley & Sons, inc., 1978)
30. F. Ajzenberg–Selove, Nucl. Phys. A **268** (1976) 1; **281** (1977) 1
31. R.K. Sheline, C.F. Liang and P. Paris, Int. J. Mod. Phys. E **3** (1994) 1267
32. S. Cwiok and W. Nazarewicz, Nucl. Phys. A **339** (1991) 95
33. A. Thiel, J. Phys. G: Nucl. Part. Phys. **16** (1990) 867
34. J.Y. Park, W. Greiner and W. Scheid, Phys. Rev. C **21** (1980) 958
35. W. Greiner, J.Y. Park and W. Scheid, in *Nuclear Molecules* (World Scientific, Singapore, 1995), chap. 11
36. M.H. Cha, J.Y. Park and W. Scheid, Phys. Rev. C **36** (1987) 2341
37. D.N. Poenaru, M. Ivaşcu, I. Ivaşcu, M. Mirea, W. Greiner, K. Depta and W. Renner, in *50 Years with Nuclear Fission*, edited by J.W. Behrens and A.D. Carlson (American Nuclear Society, Lagrange Park, 1989) pp. 617
38. N. Benfoughal and M. Mirea, J. Phys. III **6** (1996) 1403
39. M. Brack, J. Damgaard, A. Jensen, H. Pauli, V. Strutinsky and W. Wong, Rev. Mod. Phys. **44** (1972) 320
40. K.T.R. Davies and J.R. Nix, Phys. Rev. C **14** (1976) 1977
41. M.S. Ivaşcu and D.N. Poenaru, in *Particle Emission from Nuclei*, edited by D.N. Poenaru and M.S. Ivaşcu (CRC Press, Boca Raton, 1989), vol. II, Chap. 4 and 5
42. G. Audi and A.H. Wapstra, Nucl. Phys. A **565** (1993) 1
43. J.A. Wheeler, in *Niels Bohr and the Development of Physics*, edited by W.Pauli, L. Rosenfeld and W.Weisskopf (Pergamon Press, London 1955) p. 163
44. R. Blendowske, T. Fliessbach and H. Walliser, in *Nuclear Decay Modes*, edited by D.N. Poenaru (Institute of Physics Publishing, Bristol and Philadelphia, 1996), chap. 7
45. O. Serot, N. Carjan and D. Strottman, Nucl. Phys. A **569** (1994) 562
46. N. Carjan, O. Serot and D. Strottman, Z. Phys. A **349** (1994) 353